RSC Advances

ROYAL SOCIETY OF CHEMISTRY

www.rsc.org/advances

Preparation of temperature sensitive molecularly imprinted polymer coatings on nickel foam for determination of ofloxacin in Yellow River water by solid-phase microextraction

Xiujuan Guan，Xinyue Zhu，Bianfei Yu，Tong Zhao，Haixia Zhang*

State Key Laboratory of Applied Organic Chemistry, College of Chemistry and Chemical Engineering, Lanzhou University, Lanzhou 730000, China

Abstract

Nickel foam was firstly used as solid phase microextraction supporting to prepare the temperature sensitive molecularly imprinted polymers using ofloxacin as template molecules. The fluorescence intensity could be observed by naked eyes under ultraviolet light after ofloxacin adsorbing on the new materials, which was of positive proportion with the adsorbance. After adsorption occurred, significantly different fluorescence intensities distinguished the molecularly imprinted polymers from the corresponding non-molecularly imprinted polymers. A detailed evaluation was made by different characterization methods and various adsorption experiments. Finally, the molecularly imprinted polymer on nickel foam was used as adsorbent in solid phase microextraction, coupled with high performance of liquid chromatography, to detect ofloxacin, norfloxacin and enrofloxacin in the Yellow River water, obtaining recoveries from 93.2 to 108.3% and limit of quantification from 0.014 to 0.020 μg mL^{-1}.

Keywords nickel foam, molecularly imprinted polymers, fluorescence, ofloxacin

Introduction

Solid-phase microextraction (SPME) was raised as a sample pretreatment and enrichment method in 1990 and realized commercialization by Supelco company in 1993[1]. The basic formation of SPME was established including a pin support and polymer coating on quartz fiber. However, quartz fiber is too fragile and easily broken, researchers have to introduce other support types such as metal wires including stainless steel wire [2], aluminium wire [3], silver wire [4], copper wire [5], gold wire [6], platinum filament [7] and other metal oxide etc. At the same time, injector needle [8], porous material [9, 10], capillary [11], PEEK tube [12], syringe [13], electrospining [14], synthetic fiber [15, 16] and other non-metal materials [17] etc were also applied. SPME coatings are designed to expand the varieties, especially molecular imprinting polymers (MIP) bolstering their contribution [18, 19]. Other SPME modes are also developed rapidly, for example, in-tube SPME [20, 21] and stir bar SPME [22] are the common replacements now.

Nickel foam sheet (NF), a kind of porous material with suitable hardness, could be folded and cut easily. Owing to the larger specific surface area, now it is usually used in electrochemical super capacitor[23] and as electrode material[24], catalyst and sound-absorbing material. Up to now, no report was about using NF as SPME supporting.

MIP is widely used nowadays as selective adsorbent in solid phase extraction (SPE) and SPME [25, 26]. To evaluate the imprint factor of MIP, non-molecularly imprinted materials (NIP) is usually prepared simultaneously. It is difficult to distinguish the topography of NIP from MIP intuitively because the grinding destroys their topography after bulk polymerization. Even with surface polymerization, the difficulty is still existed and electron microscopy is the most effective tool for the task [27-29].

The temperature sensitive molecularly imprinted polymer coating of ofloxacin (OFL) was prepared on steel wires in our previous work [30]. The fluorescence intensity was difficult to observe from the material after trace OFL molecules adsorbed, and desorption was necessary for the quantification. Furthermore, we found the thick MIP

coating split away from steel wire easily and it was not benefit to its storage in air. To solve the problem, MIP coating was prepared on NF surface in the work (MIP-NF). The advantages of MIP-NF included: 1) stable and thinner MIP coating was obtained without losing adsorption capacity, which could be stored in air. 2) The fluorescence on MIP-NF, which could be observed by naked eyes under UV lamp, was an indicator for semiquantitative analysis of ofloxacin. 3) Different Fluorescence strength was observed on MIP-NF and NIP-NF after same absorbance procedure, which reflected intuitively the different topography of MIP and NIP on NF.

2. Experimental

2.1. Materials

OFL, enrofloxacin (ENR), norfloxacin (NOR) and sulfamerazine (SMZ) were purchased from Shanghai source biological technology Co., Ltd. (Shanghai, China). The compound structures are shown in Fig.S1 (supporting materials). 3-Methacryloxypropyltrimethoxysilane (3-MPS), N-isopropyl acryamide (NIPAAm), dopamine, methacrylate (MAA), acrylamide (AM), rhodamine B (RhB) and ethylene glycol dimethacrylate (EGDMA) were purchased from Aladdin reagent Co., Ltd. (Shanghai, China). MAA and EGDMA were used after vacuum distillation. Azodiisobutyronitrile (AIBN) was purchased from Tianjin Yuefeng Chemical Co., Ltd. (Tianjin, China) and used after recrystallization. Methanol (MeOH), ethanol (EtOH), acetone, dimethyl sulfoxide (DMSO), chloroform, acetic acid (HAc), triethylamine (TEA), Disodium hydrogen phosphate dehydrate and others were purchased from Tianjin Guangfu chemical Co., Ltd. (Tianjin, China). Phosphoric acid was purchased from Chengdu Kelong chemical Co., Ltd. (Chengdu, China). All the reagents were of analytical grade. Ultrapure water was from MILLI-Q ultrapure water system (Millipore, Bedford, MA, USA). NF (1.6 mm thickness) was purchased from Hunan Changdeliyuan Co., Ltd. (Changsha, China).

2.2. Instruments and chromatographic conditions

UV-Vis experiments were carried out on a UV-Vis spectrophotometer (TU-1810,

PUXI, Beijing). Fourier transform infrared (FTIR) spectra were acquired with a Nicolet 20 NEXUS 670 FTIR spectrophotometer (Ramsey, MA, USA) using KBr pellets; scanning electron microscope (SEM) images of materials were obtained using an S-94 4800 SEM (Hitachi, Japan). Nitrogen adsorption-desorption measurements were performed at 77K on a Ttistar ASAP 2020M Surface Area and Porosimetry analyzer (Micromeritics Instruments Corp., USA). The surface area measurement was based on the Brunauer-Emmrtt-Teller (BET) method, and the pore-size distribution was based on the Barrett-Joyner-Halenda (BEJ) formula. Thermogravimetric analysis was performed on a TGA up to 800 ℃ with a heating rate of 10 K/min in air (STA PT 1600, Linseis, Germany).

Chromatographic analysis was carried out on a high performance liquid chromatography (HPLC) system (Varian, USA) equipped with two 210 pumps, 325 UV-Vis detector, Varian star chromatographic workstation and a six-port injection valve. The HPLC operation conditions included reversed-phase C18 column (4.6×250 mm, 5 μm, Dikma technologies, Beijing, China) and mobile phase of methanol/phosphate buffer (0.01 mol L^{-1}, pH=2.70, v/v = 28/72, filtered by 0.45 μm membrane). Flow rate: 1.0 mL min^{-1}; injection: 20 μL; detection wavelength: 290 nm.

2.3 Preparation of MIPs

2.3.1 Modification of nickel foam

NF was cut into pieces of 1.5 cm × 1.5 cm, with a weight about 40 mg. The NF pieces were kept in acetone for 10 min with ultrasonic, then washed with MeOH for several times before drying.

Dried NF pieces were put into 20 mL of Tris-HCl solution (pH=8.50) containing 2 mg mL^{-1} dopamine and kept in dark for 24 h to obtain the dopamine modified NF(D-NF). After washing with methanol, The pieces of D-NF were kept in 10 mL of 3-MPS/H_2O/MeOH solution (v/v/v=1:1:8) for 30 min, followed by heating at 100℃ for 120 min. The product was washed with methanol and drying, which was named as Si-NF.

2.3.2 Synthesis of MIPs and NIPs

The MIPs were prepared according to the reference[30] with same molar ratio of

template molecule, functional monomer and cross-linking agent in same solvents. For obtaining better morphology and thinner coat of MIP, the volume of solvents was enlarged and the reaction time was shortened. Simply, in a glass test tube containing 45 mL of DMSO/ chloroform (v/v=1/2) were added 0.9 mmol of OFL, 3.15 mmol of NIPAAm and 3.6 mmol of MAA. The pre-polymerization with ultrasonic was continued for 1 h and then 1.8 mmol EGDMA, 0.24 mmol AIBN and 4 pieces of Si-NF were added in sequence. The polymerization was continued in oil bath at 70 ℃ for 6 h to obtain the MIP materials (MIP-NF).

The MIP-NF pieces were sink into 50 mL of methanol/acetic acid (97:3=v/v) with slight oscillation at 45 ℃ for 24 h to remove the template molecules (renewed the solution every 3 h). The MIP-NF pieces were kept in air until use.

The corresponding NIP materials (NIP-NF) were prepared as above in absence of OFL.

The MIP-NF materials of ENR and RhB were prepared with the same conditions. The preparation procedure was illustrated in Fig. 1.

Fig.1

2.4 Study on the adsorption properties of MIP-NF

First, the solvent used to prepare OFL solution was chosen. H_2O, ethanol and acetonitrile were used to prepare 10 mL solution with 2 μg mL^{-1} OFL, respectively. A piece of MIP-NF was kept in each solution at 25 ℃ for 24 h. The residual OFL concentration in the solutions was measured and the adsorption capacities of MIP-NF were calculated and compared with each other.

Then, the temperature sensitivity property of MIP-NF was tested. A piece of MIP-NF was immersed in 10 mL of 2 μg mL^{-1} OFL aqueous solution at 25, 35 or 45 ℃ for 24 h, respectively. After the adsorption, on the one hand, the MIP-NF was taken out and put in 10 mL water to desorb the OFL. The desorption was continued for 1 h at 25, 35 or 45 ℃, respectively, and the OFL concentration in water was determined. On the other hand, the adsorption capacities of MIP-NF at different temperature were obtained by measuring the residual OFL concentration in the adsorption solution.

Last, 10 mL aqueous solution with 0.5, 2 or 10 μg mL^{-1} OFL were prepared and in each solution was added one piece of MIP-NF to accomplish the adsorption. At different time interval from 1 to 60 min, 1 mL of the solution was taken out to measure the OFL concentrations and 1 mL water was replenished the solution to keep the volume unchanged.

All the above measures were carried out on UV-Vis spectrograph at 290 nm to get the absorbance of OFL. The adsorption amounts were calculated according to the standard curve which obeys the law of Lambert-beer. All the experiments were repeated three times and the average value was used.

2.5 The imprint factor and selectivity of MIP-NF

Each piece of NF, D-NF, Si-NF, NIP-NF and MIP-NF were put into 10 mL of OFL aqueous solution with different concentration (0.5, 1, 2, 5, 8, 10 μg mL^{-1}) to compare their adsorption capability, respectively. The static adsorption was continued for 24 h at 25 ℃. The imprint factor α was obtained by dividing the adsorption capacity (Q, μg g^{-1}) of MIP by that of NIP.

A piece of NIP-NF or MIP-NF was kept in 10 mL mixture of OFL, ENR, NOR and SMZ (each 1 μg mL^{-1}) at 25℃ for 24 h. After the adsorption, the residual concentration of each compound was calculated by their standard curves after the HPLC analysis.

2.6. Application

Using the MIP-NF as extraction adsorbent coupling with HPLC analysis, the OFL, ENR and NOR content in Yellow river water was measured.

Yellow River water was sampled from the Tanjianzi section of Yellow River in Lanzhou city. The water samples were filtered with 0.45 μm membrane and kept at 4 ℃ no more than 24 h before use.

The SPME was carried out with the following conditions: A piece of MIP-NF was put into 10 mL water sample or the samples spiking with OFL, ENR and NOR (0.025-1.0 μg mL^{-1}) , and the extraction was continued for 30 min at 25℃ with gentle shaking. The desorption of OFL from MIP-NF was repeated with 2 mL 3% acetic

acid in methanol for three times and each time continued for 5 min at 45℃. All the desorption solution was merged together and was blow-dried by nitrogen. Finally, the residual was resolved by 200 μL MeOH and 20 μL was injected for HPLC analysis.

3. Results and discussion

3.1. Preparation of materials

Temperature sensitive MIPs based on stainless steel fibers were prepared in our previous work [30]. However, a major drawback of the prepared material was fragile and the materials have to be soaked in methanol before use. Some improvements were made on the basis of previous work to solve this problem including increasing the amount of solvents and decreasing the polymerization time, and the using of NF with larger surface as supporting. In this way, the polymer layer was thin enough to prevent it from peeling off and it could be stored in the air easily.

3.2. Characterization

The SEM photographs of NF and MIP materials are shown in Fig.2. After the modification, the smooth NF surface (1,3,5 in Fig 2) was covered with granular polymers (2,4,6 in Fig 2). The NF had excellently regular morphology and could act as the qualified supporting for SPME.

The corresponding photos were obtained to trace the synthesis procedure (**Fig.S2, s**upporting materials). The color got a great change on the surface of NF. With the modification of MIP and NIP, the NF presented different colors owing to the polymers with different pores and densities, which meant it was easy to differentiate NIP and MIP with naked eyes when NF as supporting.

Fig.2

Besides IR curves of MIP and NIP materials were used to certify the successful synthesis (**Fig S3,** supporting materials), the thermogravimetric curves of the prepared materials at 0-800℃ could reflect the stability of the materials (**Fig S4,** supporting materials). The MIP lost 4.1% weight during 0-295℃ owing to the volatilization of water or other solvents. The second weight loss was in 295-450℃,

attributed to the decomposition of organic polymer. The slight different weight loss of MIP and NIP was coming from different degree of cross-link in polymers.

The results of elemental analysis are shown in **Table S1 (**supporting materials). The amount of C and N elements in MIP before and after removal of the templates are different, which proves the template molecules existing in the MIPs synthesis could be removed. After eluting the template, the caves left in MIP should be re-adsorb the template molecules from samples.

Data of N_2 adsorption is summarized in **Table S2** (supporting materials) to investigate the pore diameter ranges D_{BJH}, the pore volume V_{BJH} and the surface area S_{BET} of NIP and MIP. All the data of MIP are larger than the corresponding data of NIP. That is, MIP has larger surface area, larger pore diameter and pore volume, which is easy to understand as the results of the caves left by template molecules in MIP.

3.3 Adsorption experiments

3.3.1 Choice of solvent

The solvents used to prepare OFL solution could affect the adsorption of MIP-NF. Water, EtOH and ACN were compared in the study. The adsorption capacities were 2409, 195 and 120 μg g^{-1}, respectively. Therefore, water was chosen as the solvent to prepare OFL solution in the following experiments.

The OFL standard curve in water with UV method was obtained with the linear equation A=340.8c-36.87, R^2=0.9998 (A:absorbance, c:μg mL^{-1}).

3.3.2 Temperature sensitivity

The MIP displayed the same temperature sensitivity as the previous MIPs [30]. It meant the increase of temperature resulted in the enhanced desorption capacity and the reduced adsorption capacity, so it can be very commendable to adsorb and elute by changing temperature (Table S3, supporting materials).

3.3.3 Static adsorption

The static adsorption experiments on original NF, D-NF, Si-NF, NIP-NF and MIP-NF were accomplished at same time. No adsorption happened on the original NF, D-NF or Si-NF after 24 h (Fig 3B). Therefore, it can be concluded that all of the adsorption were due to the polymer coating. MIP-NF had about two times higher

adsorption capacities than NIP-NF when OFL concentration was not less than 2 μg mL^{-1}(α=3.2, Fig 3A). Fitting the data from experiments with Langmuir and Freundlich equations (Table S4, supporting materials), it was found that the adsorption was more corresponding to Langmuir model rather than Freundlich model.

Fig 3

3.3.4 Dynamic adsorption

The dynamic adsorption experiments showed (Fig.4) both MIP-NF and NIP-NF could get adsorption equilibrium within 30 min. Longer adsorption time was unfavorable to the adsorption capacities of MIP and the imprint factors. For example, in 10 μg mL^{-1} OFL solution, the imprint factor changed from 6.2 (30 min) to 5.2 (60 min) and to 3.2 (24 h, Fig 3). The reason was that the adsorption occurred with non-specific way initially and then with specific route into the cavities left by template molecules. Non-specific adsorption happened again after cavities were occupied entirely. Longer contact time made the latter non-specific adsorption easier, which was disadvantaged to the imprint factor.

Fig. 4

3.3.5 Fluorescence change during the adsorption procedure

The color and fluorescence change was observed during the static adsorption experiments. MIP-NF and NIP-NF were taken out after static adsorption for 24 h. Under 365 nm UV light, the fluorescence intensities of MIP-NF was enhanced with increasing OFL concentration, which was more obvious than those from NIP (**Fig.5A**). It can be explained that more OFL was combined with MIP-NF than NIP-NF. The fluorescence strength changed with the different OFL concentration, which could be used for semiquantitative analysis. Further phenomenon took place in fluorescence after these materials placed in air for another 12 h. The fluorescence intensity of MIP materials kept well but the fluorescence of NIP materials vanished (**Fig 5B**). It was speculated that the OFL molecules adsorbed on NIP materials were aggregated with the solvent evaporation, which induced fluorescence quenching. However, OFL molecules were especially adsorbed on the specific binding sites, which were regularly scattered in the MIP materials. So the fluorescence could keep no change.

The experimental phenomenon indicated a new method to identify the different structures of MIP and NIP when using NF as supporting.

In addition, the aggregation phenomenon induced fluorescence quenching was reversible. Fluorescence on NIP-NF would restore again while NIP-NF immersed into water.

Fig. 5

We prepared other two MIP-NFs using ENR and RhB as templates to verify the correctness of aggregation mechanism. The static adsorption experiments were carried out with the same conditions as those for OFL except the different concentration. The corresponding results are in the supporting materials. The fluorescence change of MIP-NF and NIP-NF of ENR were same as those of OFL (**Fig. S5,** supporting materials). The phenomena from MIP-NF and NIP-NF of RhB were a little different with those of OFL (**Fig.S6,** supporting materials). When the concentration of RhB was lower, the same phenomena as those of OFL were obtained. Higher RhB concentration caused larger adsorption amount, which brought not only the fluorescence on MIP-NF and NIP-NF much brighter but also the obvious color presented (**Fig S7**, supporting materials). The different phenomena of RhB from OFL might be resulted from the strong adsorption property of RhB and its bright color, which disturbed the observation of fluorescence.

3.3.6 Competitive adsorption experiment

Several antibiotics were used to evaluate the selectivity of MIP materials. It can be seen that MIP-NF had much better adsorption capacity to the antibiotics than SMZ (**Fig. 6**). OFL had the largest adsorption capacity and highest imprint factor α among the antibiotics studied.

Fig.6

3.4 Application

The MIP-NF was used to determine the antibiotics in Yellow River water coupling with HPLC under the optimal extraction conditions. Desorption condition was then optimized. Normally a mixture of organic solvent and acid was used[30]. We compared the desorption results from different contents of acetic acid (1%, 3% and

10%) in methanol as eluent. Higher acetic acid concentration (10%) could destroy the nickel foam and 1% acetic acid could not desorb the molecules effectively. So 3 % acetic acid in methanol was adopted in this experiment. The desorption volume and times were investigated too and the results showed that 3×200 μL could elute more than 90% OFL from the MIP-NF.

The linear scope, standard curve, limit of detection (LOD_{LC}, the signal-to-noise ratio (S/N) ratio of 3:1) and quantification (LOQ_{LC}, the least amount could be quantified) was summarized in Table 1. Recoveries and RSD% was in Table 2. It could be found that the satisfied recoveries (from 93.2-108.3%) were obtained. The LOQ_{LC} of OFL, NOR and ENR was 0.020, 0.015 and 0.014 μg mL^{-1}, respectively. The LOQ_{LC} of OFL was twice lower than the previous result on steel wire[30], which verified the benefit using NF as supporting. Chromatograms of the standard addition of the three antibiotics in Yellow River water (25 ng mL^{-1}) are shown in Fig. 7. No antibiotics were found in the sample. Compared the chromatographic peaks in (B, 0.25μg mL^{-1}, direct injection) with (C, 0.025μg mL^{-1}, after MIP-NF treatment), the enrichment efficiency was satisfied.

Fig. 7

4. Conclusion

A new MIP of ofloxacin with nickel foam as supporting was obtained through modification of dopamine, silane and a thin MIP coating in sequency. After adsorption of ofloxacin, the MIP on nickel foam showed the obvious fluorescence, which could do semiquantitative analysis directly. The different fluorescence change between MIP and NIP, caused by the aggregation induced fluorescence quenching, reflected their different topology and the different kind of adsorption sites on MIP and NIP. The MIP material on nickel foam owns the good selectivity, better adsorption capacity and simple SPME operation.

Acknowledges

The authors thank the funding from Gansu Province Science and Technology Support Program (1204FKCA127) and the National Science Foundation of China (21375052)

References

1. C. L. Arthur and J. Pawliszyn, *Analytical chemistry*, 1990, **62**, 2145-2148.
2. X. Hu, G. Dai, J. Huang, T. Ye, H. Fan, T. Youwen, Y. Yu and Y. Liang, *Journal of Chromatography A*, 2010, **1217**, 5875-5882.
3. D. Djozan, B. Ebrahimi, M. Mahkam and M. A. Farajzadeh, *Analytica chimica acta*, 2010, **674**, 40-48.
4. B. B. Prasad, M. P. Tiwari, R. Madhuri and P. S. Sharma, *Journal of Chromatography A*, 2010, **1217**, 4255-4266.
5. P. Hashemi, M. Shamizadeh, A. Badiei, P. Z. Poor, A. R. Ghiasvand and A. Yarahmadi, *Analytica chimica acta*, 2009, **646**, 1-5.
6. M. Mattarozzi, M. Giannetto, A. Secchi and F. Bianchi, *Journal of Chromatography A*, 2009, **1216**, 3725-3730.
7. W. Du, F. Zhao and B. Zeng, *Journal of Chromatography A*, 2009, **1216**, 3751-3757.
8. M. M. Moein, D. Jabbar, A. Colmsjö and M. Abdel-Rehim, *Journal of Chromatography A*, 2014, **1366**, 15-23.
9. Z. Zhang, Q. Wang and G. Li, *Analytica chimica acta*, 2012, **727**, 13-19.
10. J. Yang, Y. Li, J. Wang, X. Sun, S. M. Shah, R. Cao and J. Chen, *Analytica chimica acta*, 2015, **853**, 311-319.
11. F. Tan, H. Zhao, X. Li, X. Quan, J. Chen, X. Xiang and X. Zhang, *Journal of Chromatography A*, 2009, **1216**, 5647-5654.
12. J. Zhang, W. Zhang, T. Bao and Z. Chen, *Journal of Chromatography A*, 2015, **1388**, 9-16.
13. M. García-Valverde, R. Lucena, F. Galán-Cano, S. Cárdenas and M. Valcárcel, *Journal of Chromatography A*, 2014, **1343**, 26-32.
14. S. Chigome and N. Torto, *TrAC Trends in Analytical Chemistry*, 2012, **38**, 21-31.
15. E. M. Reyes-Gallardo, R. Lucena, S. Cárdenas and M. Valcárcel, *Journal of Chromatography A*, 2014, **1345**, 43-49.
16. V. Samanidou, L.-D. Galanopoulos, A. Kabir and K. G. Furton, *Analytica chimica acta*, 2015, **855**, 41-50.
17. Y.-B. Luo, B.-F. Yuan, Q.-W. Yu and Y.-Q. Feng, *Journal of Chromatography A*, 2012, **1268**, 9-15.
18. X. Hu, Y. Fan, Y. Zhang, G. Dai, Q. Cai, Y. Cao and C. Guo, *Analytica chimica acta*, 2012, **731**, 40-48.
19. J. Gauczinski, Z. Liu, X. Zhang and M. Schönhoff, *Langmuir*, 2012, **28**, 4267-4273.
20. S. Xu, X. Zhang, Y. Sun and D. Yu, *Analyst*, 2013, **138**, 2982-2987.
21. M. Mei, X. Huang and D. Yuan, *Journal of Chromatography A*, 2014, **1345**, 29-36.
22. J. Aguirre, E. Bizkarguenaga, A. Iparraguirre, L. Á. Fernández, O. Zuloaga and A. Prieto,

Analytica chimica acta, 2014, **812**, 74-82.

23. L. Gu, Y. Wang, R. Lu, L. Guan, X. Peng and J. Sha, *Journal of Materials Chemistry A*, 2014, **2**, 7161-7164.
24. H. Wang, G. Wang, Y. Ling, F. Qian, Y. Song, X. Lu, S. Chen, Y. Tong and Y. Li, *Nanoscale*, 2013, **5**, 10283-10290.
25. F. Ning, H. Peng, J. Li, L. Chen and H. Xiong, *Journal of agricultural and food chemistry*, 2014, **62**, 7436-7443.
26. S. Farzaneh, E. Asadi, M. Abdouss, A. Barghi-Lish, S. Azodi-Deilami, H. A. Khonakdar and M. Gharghabi, *RSC Advances*, 2015, **5**, 9154-9166.
27. W. Ji, L. Chen, X. Ma, X. Wang, Q. Gao, Y. Geng and L. Huang, *Journal of Chromatography A*, 2014, **1342**, 1-7.
28. Z. Xu, Z. Yang and Z. Liu, *Journal of Chromatography A*, 2014, **1358**, 52-59.
29. X. Liu, Z. Chen, J. Long, H. Yu, X. Du, Y. Zhao and J. Liu, *Industrial & Engineering Chemistry Research*, 2014, **53**, 16082-16090.
30. T. Zhao, X. Guan, W. Tang, Y. Ma and H. Zhang, *Analytica chimica acta*, 2015, **853**, 668-675.

Captions

Fig.1. Schematic diagram of MIP-NF synthesis

Fig.2. Scanning electron micrographs of NF (1, 3, 5) and MIP-NF (2, 4, 6): (1, 2)×30，(3, 4)×120 (5, 6)×1500

Fig.3. Adsorption isotherms of OFL on different materials

(a) MIP-NF; (b) NIP-NF; (c) NF; (d) D-NF; (e) Si-NF.

Conditions: adsorption temperature: 25℃; adsorption time: 24 h; samples: 10 mL OFL aqueous solutions with different concentrations.

Fig.4. Adsorption kinetic curves of OFL on MIP-NF (M) and NIP-NF (N)

Conditions: adsorption temperature: 25℃; samples: 10 mL OFL aqueous solutions with different concentrations (0.5, 2, 10 μg mL^{-1}). M meant MIP and N meant NIP.

Fig.5. Photos of MIP-NF (M) and NIP-NF (N) under ultraviolet lamp after static adsorption of OFL for 24 h (A) and in air for another 12 h (B).

Conditions: adsorption temperature 25℃; samples: 10 mL OFL aqueous solutions with different concentrations (1-6 were 0.5, 1, 2, 5, 8, 10 μg mL^{-1}, respectively).

Fig.6. Adsorption of different compounds on MIP-NF and NIP-NF

Conditions: adsorption temperature: 25℃; adsorption time: 24 h; samples: 10 mL aqueous solutions with 2 μg mL^{-1} of OFL (or ENR or NOR or SMZ).

Fig.7. Chromatograms of Yellow River water samples

Yellow River water samples treated with MIP-NF without (A) and with (C) spiked with 0.025 μg mL^{-1} of each standard compound. (B）direct injection of the standard with 0.25μg mL^{-1} of each compound. OFL (1); ENR (2); NOR (3).

HPLC conditions: stationary phase: C18; mobile phase: solvent A ((0.01 mol L^{-1} phosphate buffer, pH=2.70) and solvent B (MeOH), A/B=72:28. Flow rate: 1 mL min^{-1}; injection: 20 μL; detection wavelength: 290 nm.

Table 1 The correlation coefficient, LOD and LOQ of three analytes (n=3)

Compound	linear equation	Linear scope (ng mL^{-1})	R^2	LOD (ng mL^{-1})	LOQ (ng mL^{-1})
OFL	Y=51.38X+13.66	20-50000	0.9998	6.021	20.02
NOR	Y=106.4X-12.30	15-50000	0.9999	4.451	14.84
ENR	Y=112.0X-28.61	14-50000	0.9999	4.229	14.10

Table 2 Performance of MIP –HPLC methods for Yellow River water (n=3)

Added	Recovery (%)			Intra RSD (%)			Inter RSD (%)		
Concentration (μg mL^{-1})	OFL	NOR	ENR	OFL	NOR	ENR	OFL	NOR	ENR
0.05	109.6	93.2	98.2	5.06	4.43	3.48	5.87	4.74	5.11
1	96.9	108.3	100.1	6.52	3.43	5.54	3.61	3.61	3.62
5	99.9	100.9	101.3	6.02	4.42	4.54	3.52	3.52	1.2

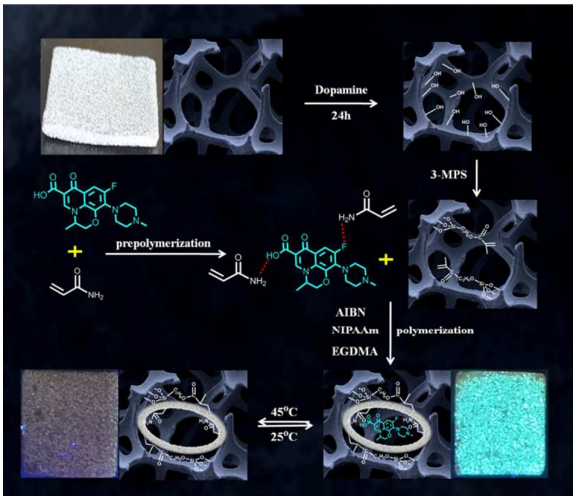

Fig.1.

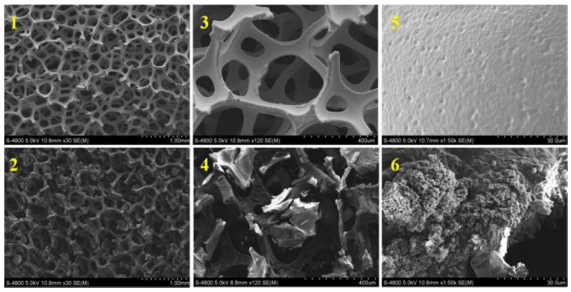

Fig.2.

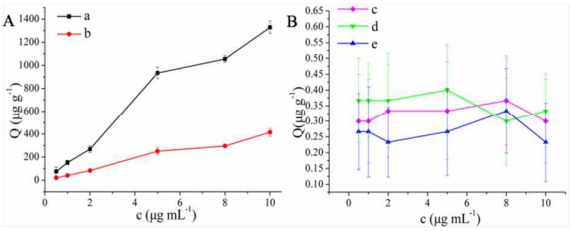

Fig.3.

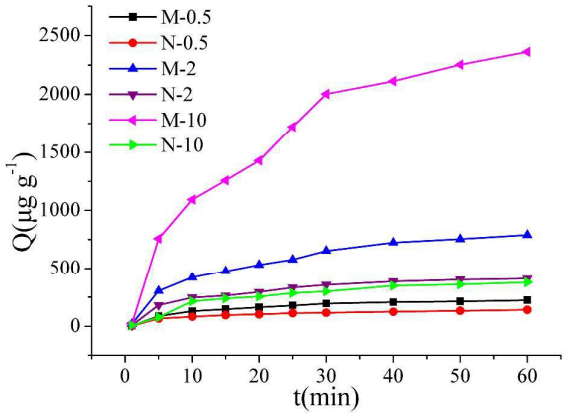

Fig 4

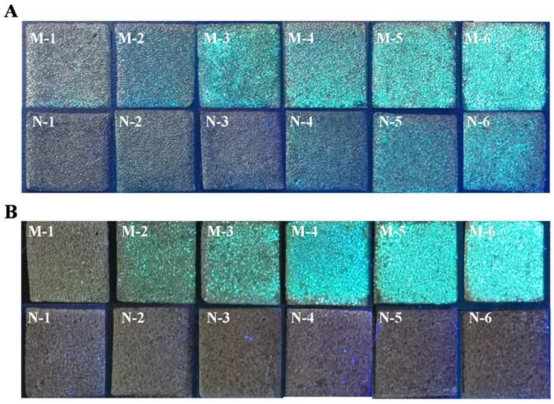

Fig.5.

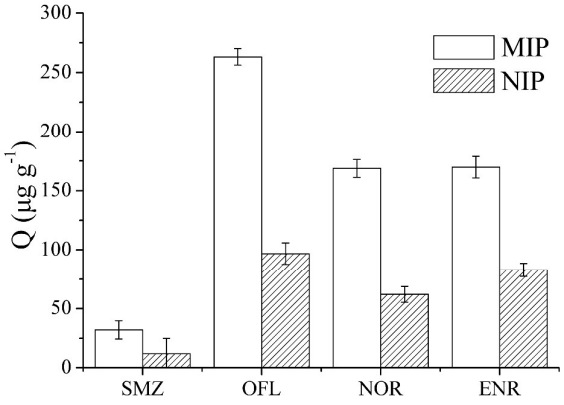

Fig.6.

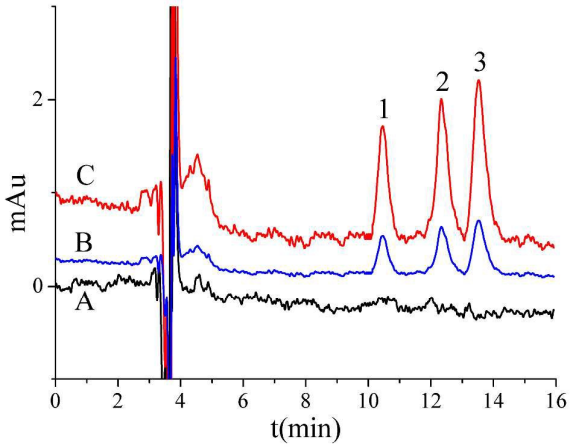

Fig.7.